

# Toward dynamic isotopomer analysis in the rat brain *in vivo*: automatic quantitation of $^{13}\text{C}$ NMR spectra using LCMoDel

Pierre-Gilles Henry,<sup>1\*</sup> Gülin Öz,<sup>1</sup> Stephen Provencher<sup>3</sup> and Rolf Gruetter<sup>1,2</sup>

<sup>1</sup>Department of Radiology, Center for Magnetic Resonance Research, University of Minnesota Medical School, Minneapolis, MN 55455, USA

<sup>2</sup>Department of Neuroscience, Center for Magnetic Resonance Research, University of Minnesota Medical School, Minneapolis, MN 55455, USA

<sup>3</sup>48 Chancery Lane East, Oakville, Ontario Canada, L6J 5P6

Received 3 July 2003; Revised 11 August 2003; Accepted 12 August 2003

**ABSTRACT:** The LCMoDel method was adapted to analyze localized *in vivo*  $^{13}\text{C}$  NMR spectra obtained from the rat brain *in vivo* at 9.4 T. Prior knowledge of chemical-shifts,  $J$ -coupling constants and  $J$ -evolution was included in the analysis. Up to 50 different isotopomer signals corresponding to 10 metabolites were quantified simultaneously in 400  $\mu\text{l}$  volumes in the rat brain *in vivo* during infusion of  $[1,6\text{-}^{13}\text{C}_2]\text{glucose}$ . The analysis remained accurate even at low signal-to-noise ratio of the order of 3:1. The relative distribution of isotopomers in glutamate, glutamine and aspartate determined *in vivo* in 22 min was in excellent agreement with that measured in brain extracts. Quantitation of time series of  $^{13}\text{C}$  spectra yielded time courses of total  $^{13}\text{C}$  label incorporation into up to 16 carbon positions, as well as time courses of individual isotopomer signals, with a temporal resolution as low as 5 min (dynamic isotopomer analysis). The possibility of measuring *in vivo* a wealth of information that was hitherto accessible only in extracts is likely to expand the scope of metabolic studies in the intact brain. Copyright © 2003 John Wiley & Sons, Ltd.

**KEYWORDS:**  $^{13}\text{C}$  NMR spectroscopy; *in vivo*; brain; quantitation; LCMoDel; prior knowledge; isotopomers

## INTRODUCTION

*In vivo*  $^{13}\text{C}$  NMR spectroscopy combined with the administration of  $^{13}\text{C}$ -enriched substrates is a unique tool to investigate brain metabolism. The high chemical specificity of  $^{13}\text{C}$  NMR, which can distinguish  $^{13}\text{C}$  isotope incorporation not only into different molecules, but also into specific carbon positions within the same molecule ( $^{13}\text{C}$  isotopomers), allows the fate of  $^{13}\text{C}$  label to be followed through multiple metabolic pathways.<sup>1</sup> In contrast to studies performed on brain extracts, where the multiplet structure of  $^{13}\text{C}$  NMR resonances caused by  $^{13}\text{C}$ – $^{13}\text{C}$  scalar couplings was exploited,<sup>2</sup> the amount of information accessible in the brain *in vivo* has been limited by the lower signal-to-noise ratio and the lower spectral resolution of *in vivo* spectra.

Recent improvements in direct, localized  $^{13}\text{C}$  NMR spectroscopy have considerably expanded the amount of information that can be obtained *in vivo* in the human brain<sup>3–7</sup> and in the rat brain.<sup>8–10</sup> The availability of higher field magnets, the use of automated shimming procedures<sup>11</sup> and more efficient second-order shim coils, and the development of new pulse sequences for localized detection<sup>3,6,8,9</sup> have led to substantial gains in sensitivity, spectral resolution and localization performance (see also the review by Gruetter *et al.* in this issue). Broadband  $^1\text{H}$ -localized  $^{13}\text{C}$  spectra obtained recently from the rat brain at 9.4 T during an infusion of  $^{13}\text{C}$ -labeled glucose have allowed the detection of  $^{13}\text{C}$  NMR signals from 18 different carbon positions, ranging from the alanine C3 resonance at 17 ppm to the glucose C1 $\beta$  resonance at 96.8 ppm.<sup>8</sup> In addition, the fine structure arising from  $^{13}\text{C}$ – $^{13}\text{C}$   $J$ -couplings became detectable not only in glutamate,<sup>4,9</sup> but in several other metabolites, suggesting that numerous isotopomers could be measured in the brain *in vivo* with a temporal resolution suitable for dynamic isotopomer analysis.

Quantitative analysis of *in vivo*  $^{13}\text{C}$  spectra has traditionally been performed using manual peak integration or peak fitting of individual resonances.<sup>10,12,13</sup> This approach, although user-dependent and time-consuming, is often adequate because *in vivo*  $^{13}\text{C}$  NMR spectra are typically characterized by a high spectral dispersion and a flat baseline (provided that lipid signals coming from the

\*Correspondence to: P.-G. Henry, Center for Magnetic Resonance Research, 2021 6th St SE, Minneapolis, MN 55455, USA.

E-mail: henry@cmrr.umn.edu

Contract/grant sponsor: NIH; contract grant number: R01NS38672.

Contract/grant sponsor: Whitaker Foundation.

**Abbreviations used:** The notation adopted in this paper for  $^{13}\text{C}$  isotopomers is defined in the Methods. Ala, alanine; Asp, aspartate; Cr, creatine; CRLB, Cramer–Rao lower bound; DEPT, distortionless enhancement by polarization transfer; GABA, gamma amino-butyric acid; Glc, glucose; Gln, glutamine; Glu, glutamate; IE, isotopic enrichment; Lac, lactate; *myo*-Ins, *myo*-inositol; NAA, *N*-acetyl-aspartate;  $V_{\text{pdh}}$ , rate of the tricarboxylic acid cycle;  $V_x$ , rate of exchange between 2-oxoglutarate and glutamate.

scalp are properly eliminated, either by spatial localization of NMR signals, or by subtraction of a natural abundance background spectrum acquired before infusion of  $^{13}\text{C}$ -labeled substrate). However, even with excellent shimming and spatial localization of NMR signals, quantitation of multiplets arising from different  $^{13}\text{C}$  isotopomers remains challenging in the brain *in vivo* because of the low signal-to-noise ratio and because the linewidth of  $^{13}\text{C}$  singlets (typically 5–10 Hz depending on  $B_0$  field strength and shimming) is not negligible compared with homonuclear  $^{13}\text{C}$ – $^{13}\text{C}$   $J$ -coupling values (30–50 Hz), leading to significant overlap of multiplets within a given carbon resonance.

Incorporation of prior knowledge has been shown to improve the precision of spectral analysis, especially in the presence of spectral overlap.<sup>14–16</sup> Of the numerous methods that have been proposed to analyze NMR spectra, either in the time domain<sup>17</sup> or in the frequency domain,<sup>18</sup> several have the capability to incorporate prior knowledge.<sup>19–23</sup> Prior knowledge has been used to quantify, for example,  $^{13}\text{C}$ – $^{13}\text{C}$  multiplets from tissue extracts,<sup>24–27</sup>  $^2\text{H}$ – $^{13}\text{C}$  multiplets from cell suspensions,<sup>19</sup> *in vivo*  $^{13}\text{C}$  spectra from muscle<sup>28</sup> or C1-glycogen and C1-glucose signals in  $^{13}\text{C}$  spectra from perfused liver,<sup>29</sup> but to the best of our knowledge such an approach has not been reported for quantitation of  $^{13}\text{C}$  isotopomers in the brain *in vivo*.

LCModel<sup>23</sup> (linear combination of model spectra) has become increasingly popular to quantify *in vivo*  $^1\text{H}$  NMR spectra (for a recent review see Provencher<sup>30</sup>) and has been used extensively in our laboratory.<sup>31–33</sup> LCModel has several attractive features for analysis of *in vivo* spectra: a model-free lineshape, a high degree of flexibility in the introduction of prior knowledge, and robustness in cases of low signal-to-noise ratio and spectral overlap. Furthermore, the program is fully automatic, another advantage for processing time series of  $^{13}\text{C}$  spectra. However, because LCModel was originally designed for the analysis of  $^1\text{H}$  spectra, specific assumptions were made regarding the information content of the data to be fitted, such as the presence of substantial singlet signals (e.g. NAA or Cr) in the spectrum for the preliminary determination of lineshape, as well as a small spectral range (a few ppm). These and other assumptions required significant adjustments in order to apply the original LCModel program to *in vivo*  $^{13}\text{C}$  NMR spectra.

The purpose of this work was (1) to adapt LCModel for the analysis of *in vivo*  $^{13}\text{C}$  NMR spectra using prior knowledge, and (2) to evaluate the feasibility and robustness of dynamic  $^{13}\text{C}$  isotopomers analysis in the rat brain *in vivo*.

## MATERIALS AND METHODS

### Animal preparation

All animal experiments were performed in accordance with the guidelines for the care and use of laboratory

animals and were approved by the Institutional Animal Care and Use Committee of the University of Minnesota. Male Sprague–Dawley rats ( $n = 5$ ; weight  $273 \pm 23$  g, mean  $\pm$  SD) (Harlan, Indianapolis, IN, USA) were intubated and ventilated with a 70%:30%  $\text{N}_2\text{O}$ – $\text{O}_2$  mixture and 3% isoflurane. Both femoral veins were cannulated for the i.v. administration of glucose and  $\alpha$ -chloralose, and both arteries were cannulated for blood sampling to monitor blood gases and plasma glucose concentrations. Immediately after surgery, isoflurane was discontinued and replaced by intravenous  $\alpha$ -chloralose administration (bolus 40 mg/kg, then continuous infusion at 25.4 mg/kg/h). Animals were placed prone in a home-built holder and the head position was fixed using ear rods and a bite-bar. After adjustment of NMR parameters, a bolus of 99%-enriched [1,6- $^{13}\text{C}_2$ ]glucose (Cambridge Isotope Laboratories) was administered over 5 min with an infusion rate decaying exponentially every minute. This bolus was followed by a continuous infusion of 70%-enriched glucose for the remaining 7 h of the experiment. Small adjustments were made to the rate of continuous infusion to keep plasma glucose around 300 mg/dl. This protocol was optimized to achieve a stable plateau in plasma glucose isotopic enrichment.<sup>34</sup>

### *In vivo* $^{13}\text{C}$ NMR spectroscopy

All *in vivo* spectra were acquired on a 9.4 T/31 cm bore magnet (Magnex Scientific, Oxford, UK) interfaced to an Inova console (Varian, Palo Alto, CA, USA). The magnet was equipped with gradients reaching 300 mT/m in 500  $\mu\text{s}$  and with a set of custom-designed second-order shim coils capable of producing shim strengths up to 0.05 mT/cm<sup>2</sup> (Magnex Scientific, Oxford, UK). The coil assembly consisted of a  $^1\text{H}$  quadrature surface coil (two loops of 14 mm diameter) and an inner  $^{13}\text{C}$  linearly polarized surface coil (12 mm diameter) built according to a previously described design.<sup>35</sup> Spin-echo RARE images were acquired to select a  $9 \times 5 \times 9$  mm<sup>3</sup> volume in the rat brain. Adjustment of all first and second-order shims using FAST(EST)MAP<sup>11</sup> resulted in an 18–23 Hz water linewidth in the 400  $\mu\text{l}$  voxel. Localized *in vivo*  $^{13}\text{C}$  NMR spectra were acquired with a semi-adiabatic DEPT sequence as described elsewhere.<sup>8</sup> Briefly, localization was performed on the  $^1\text{H}$  magnetization using 3D-ISIS combined with outer volume saturation (OVS). Magnetization was then transferred to  $^{13}\text{C}$  using gradient-spoiled semi-adiabatic DEPT polarization transfer. The interpulse delay was 3.8 ms (optimized for  $J_{\text{CH}} = 130$  Hz) and the nominal flip angle of the last  $^1\text{H}$  pulse was set to 45° in order to detect signals from CH, CH<sub>2</sub> and CH<sub>3</sub> groups simultaneously. Repetition time was 2.5 s. WALTZ-16 composite pulse decoupling was applied during the acquisition time (205 ms, 8192 complex points) with a nominal  $\gamma B_1/2\pi$  of 2 kHz.

## <sup>13</sup>C NMR spectroscopy of brain extracts

At the end of the *in vivo* measurements, brains were funnel-frozen *in situ* with liquid nitrogen<sup>36,37</sup> as follows. Animals were deeply anesthetized with an i.v. bolus of pentobarbital (25 mg/kg) and the scalp was quickly retracted. A funnel was applied directly on the skull and application of liquid nitrogen resulted in frozen brain within 2 min, at which point the animals were decapitated. A final blood sample was taken 1 min after starting funnel-freezing to ensure that mechanical ventilation maintained adequate blood oxygenation. The brain was dissected out of the skull under intermittent liquid nitrogen to minimize post-mortem metabolism. Brain tissue was crushed in a mortar and pestle and extracted with 5 ml ice-cold perchloric acid (0.9 M). Samples were centrifuged for 15 min at 4°C and the supernatant was neutralized with 9 M KOH. After another 15 min centrifugation, supernatants were freeze-dried and resuspended in 10% D<sub>2</sub>O–90% H<sub>2</sub>O and pH was adjusted to 7.15 ± 0.05 (range 7.1–7.2; *n* = 5) by titration with 1 M HCl or 1 M NaOH. This pH was close to pH values reported in the rat brain.<sup>38</sup> The effect of 10% D<sub>2</sub>O on measurements of pH using a glass electrode was shown to be less than 0.04 pH units.<sup>39</sup>

Perchloric acid extracts of brain tissue were measured using high-resolution <sup>13</sup>C NMR spectroscopy on a 14.1 T Varian Unity Inova spectrometer. One-dimensional pulse-acquire <sup>13</sup>C spectra were acquired with NOE under fully relaxed conditions (*TR* = 15 s, spectral width 30 000 Hz, acquisition time 1 s, with WALTZ-16 decoupling). All resonances were fitted using built-in spectrometer software after zero-filling to 512 K points. Resonance frequencies measured in spectra from five different animals were used to determine mean chemical-shifts and *J*-coupling values. Assignment of resonances was based on peak position using published values<sup>24,41–43</sup> (Rogers Magnetic Resonance Center [http://www2.utsouthwestern.edu/rogersmr/chemical\\_shifts.htm](http://www2.utsouthwestern.edu/rogersmr/chemical_shifts.htm); W. Wilker; [http://alf.zfn.uni-bremen.de/~wie/www\\_metab.html](http://alf.zfn.uni-bremen.de/~wie/www_metab.html)) and on relative signal intensity. All chemical-shift values were referenced to lactate at 21 ppm.

## LCModel data processing

*In vivo* spectra were processed using a modified version of LCModel 2.3 (Stephen Provencher Inc., Oakville, Ontario, Canada). Input files for LCModel were generated automatically using Matlab (The MathWorks Inc., Natick, MA, USA). FIDs were preprocessed to place the center of the spectral window at 4.65 ppm by applying a linear phase shift in the time domain after removing the DC offset. No other baseline correction, zero-filling or time-domain filtering was applied prior to LCModel analysis. Because LCModel was initially designed to analyze <sup>1</sup>H spectra, significant changes had to be made in the input

parameters in the CONTROL input file (see Appendix for the most important parameters). Spectra were processed using a Sun Blade 2000 64-bit workstation (Sun Microsystems, Santa Clara, CA, USA) equipped with two 900 MHz copper processors. The typical time required for analysis of one broadband <sup>13</sup>C spectrum was 4 min.

The basis set for LCModel was generated using Matlab by simulating each isotopomer with the appropriate chemical-shift and *J*-coupling pattern (based on the values measured in this study). For isotopomers labeled at more than one carbon, homonuclear <sup>13</sup>C–<sup>13</sup>C *J*-modulation occurring during the delay 2\* $\tau$  [where  $\tau = 1/(2*J_{CH})$  and  $J_{CH} = 130$  Hz] between <sup>13</sup>C excitation (i.e. the first segment of the BIR-4 pulse) and acquisition in the DEPT sequence was taken into account by simulating the corresponding phase distortion of the multiplet spectrum assuming weak coupling conditions. For example, the triplet of glutamate C3 at 27.84 ppm was simulated as the sum of three lines with relative intensities 1:2:1, relative frequencies  $-J_{CC}:0:J_{CC}$  (in this case  $J_{CC} = 34.6$  Hz) and relative phases  $\phi_0:0:-\phi_0$  with  $\phi_0 = 2\pi*\tau*J_{CC}$  radians. The delay  $\tau$  used to calculate  $\phi_0$  was empirically set to 2.75 ms, which was shorter than  $1/(2*J_{CH})$ , because <sup>13</sup>C–<sup>13</sup>C *J*-modulation was reduced during the high  $B_1$  part of the segmented BIR-4 pulse (2 ms total duration). In cases where one of the two coupled carbons belonged to a carboxyl group (COOH), *J*-modulation was neglected because carboxyl carbon resonances (e.g. the C1 of glutamate at ~175 ppm) were not inverted by the middle segment of the BIR-4 pulse. In all cases the lineshape for the basis set was Lorentzian with 4 Hz full-width at half-maximum. In addition, a small singlet was added at 0 ppm in all basis spectra for automatic frequency referencing. About 50 different isotopomer resonances were included in the basis set, as listed in Table 1. Relative concentrations determined by LCModel were converted into absolute concentrations (in  $\mu\text{mol/g}$  wet weight) using the fractional enrichment of glutamate C4 measured on extracts and assuming a glutamate concentration of 10  $\mu\text{mol/g}$ . Correction factors were applied to account for differences in polarization transfer efficiency and off-resonance effects across the <sup>13</sup>C spectrum.

## Notation

The notation adopted here for <sup>13</sup>C multiplets was similar to that used by Jeffrey *et al.*<sup>26</sup> A specific multiplet was designated by an abbreviation of the metabolite name, followed by the specific carbon resonance observed, then by a letter denoting the multiplet structure (S = singlet, D = doublet, T = triplet, DD = doublet of doublet). For example, Glu-C3S and Glu-C3T designated the singlet and the triplet of glutamate at the C3 position. To indicate the total amount of <sup>13</sup>C label at a specific carbon position, the resonance name was used without any additional letter. Thus Glu-C3 referred to the sum of all glutamate isotopomers labeled at the C3 position. In some cases it

was necessary to further specify which doublet was considered by adding two numbers to indicate the  $J$ -coupling. For example, Glu-C2D21 and Glu-C2D23 designated two different doublets at the C2 position, one corresponding to the coupling to the C1, the other to the coupling to the C3. When the coupling constants were identical, no numbers were added. Therefore Glu-C3D actually was the sum of Glu-C3D32 and Glu-C3D34. Note that a given multiplet can represent the sum of different  $^{13}\text{C}$  isotopomers. For example, Glu-C3T =  $[2,3,4-^{13}\text{C}_3]\text{glutamate} + [1,2,3,4-^{13}\text{C}_4]\text{glutamate} + [2,3,4,5-^{13}\text{C}_4]\text{glutamate}$ . Long-range couplings are small (typically 1 Hz for two-bond couplings and 2–3 Hz for three-bond couplings<sup>44</sup>) compared with the linewidth of  $^{13}\text{C}$  resonances observed *in vivo*, and their effect on linewidth and lineshape was assessed to be negligible in this study.

## Statistics

Signal-to-noise ratios were calculated as the peak height divided by twice the root mean square noise. All results are provided as mean  $\pm$  SD.

## RESULTS

*In vivo*  $^{13}\text{C}$  NMR spectra obtained from the rat brain at 9.4 T contained a considerable amount of information [Fig. 1(a)] as in our previous study.<sup>8</sup> Resonances from glucose C1, glucose C6, glutamate C4, C3, C2, glutamine C4, C3, C2 and aspartate C3, C2 were detected, as well as smaller resonances from GABA, NAA and lactate. *In vivo* spectra were in appearance very similar to appropriately line-broadened spectra obtained from brain extracts [Fig. 1(b)]. The funnel-freezing procedure resulted in relatively high brain glucose and low lactate concentrations detected in  $^{13}\text{C}$  spectra of brain extracts.

Chemical shifts and homonuclear  $J$ -coupling constants were measured in extract spectra obtained from five different animals after 7 h of  $[1,6-^{13}\text{C}_2]\text{glucose}$  infusion (Fig. 2). Multiplets were detected for glucose C1, glucose C6, glutamate and glutamine C2, NAA and aspartate C2, GABA C4 and NAA C3, aspartate C3, GABA C2 and glutamate C4, glutamine C4, glutamate and glutamine C3, and GABA C3. These multiplets were in general the superposition of spectral contributions from different isotopomers. For example, the multiplet corresponding to the glutamate C3 resonance at 27.85 ppm was the sum of a singlet Glu-C3S, a doublet Glu-C3D (corresponding

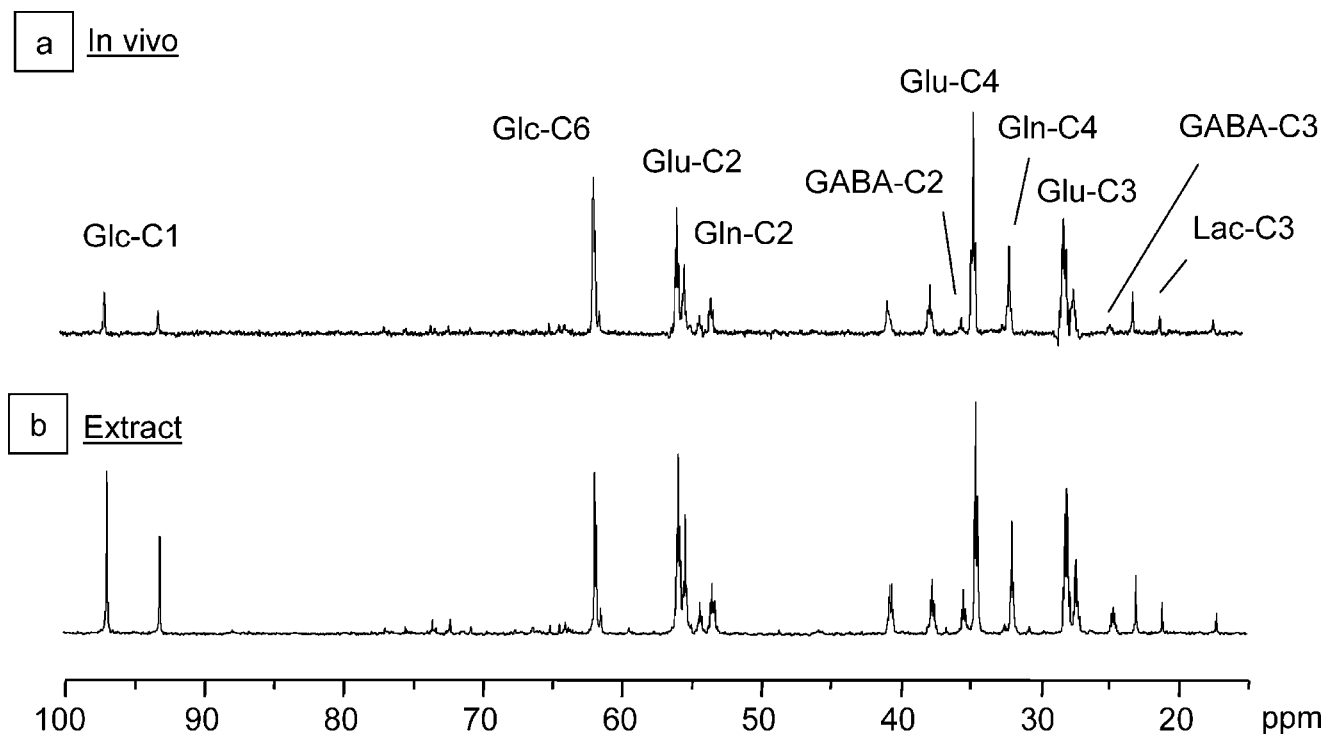


**Figure 1.** Comparison of  $^{13}\text{C}$  NMR spectra acquired *in vivo* and from brain extracts: (a)  $^1\text{H}$ -localized  $^{13}\text{C}$  spectrum acquired from the rat brain (400  $\mu\text{l}$ ) 3 h after starting an infusion of  $[1,6-^{13}\text{C}_2]\text{glucose}$  (5120 scans,  $TR$  2.5s); (b) High-resolution  $^{13}\text{C}$  spectrum from a perchloric acid extract of brain tissue acquired at 150 MHz (256 scans,  $TR$  15 s, with NOE enhancement). Minimal post-mortem degradation was present, as judged from the high glucose C6 signal and the low lactate C3 signal. The extract spectrum was line-broadened (8 Hz Lorentzian line broadening) to match the linewidth of the processed *in vivo* spectrum (3 Hz line broadening). The lower intensity of glucose C1 on the *in vivo* spectrum is due to off-resonance effects of the pulse sequence. Note the phase distortion of  $^{13}\text{C}$ – $^{13}\text{C}$  multiplets *in vivo*, especially visible for glutamate C3 around 27.9 ppm, due to  $^{13}\text{C}$ – $^{13}\text{C}$   $J$ -modulation

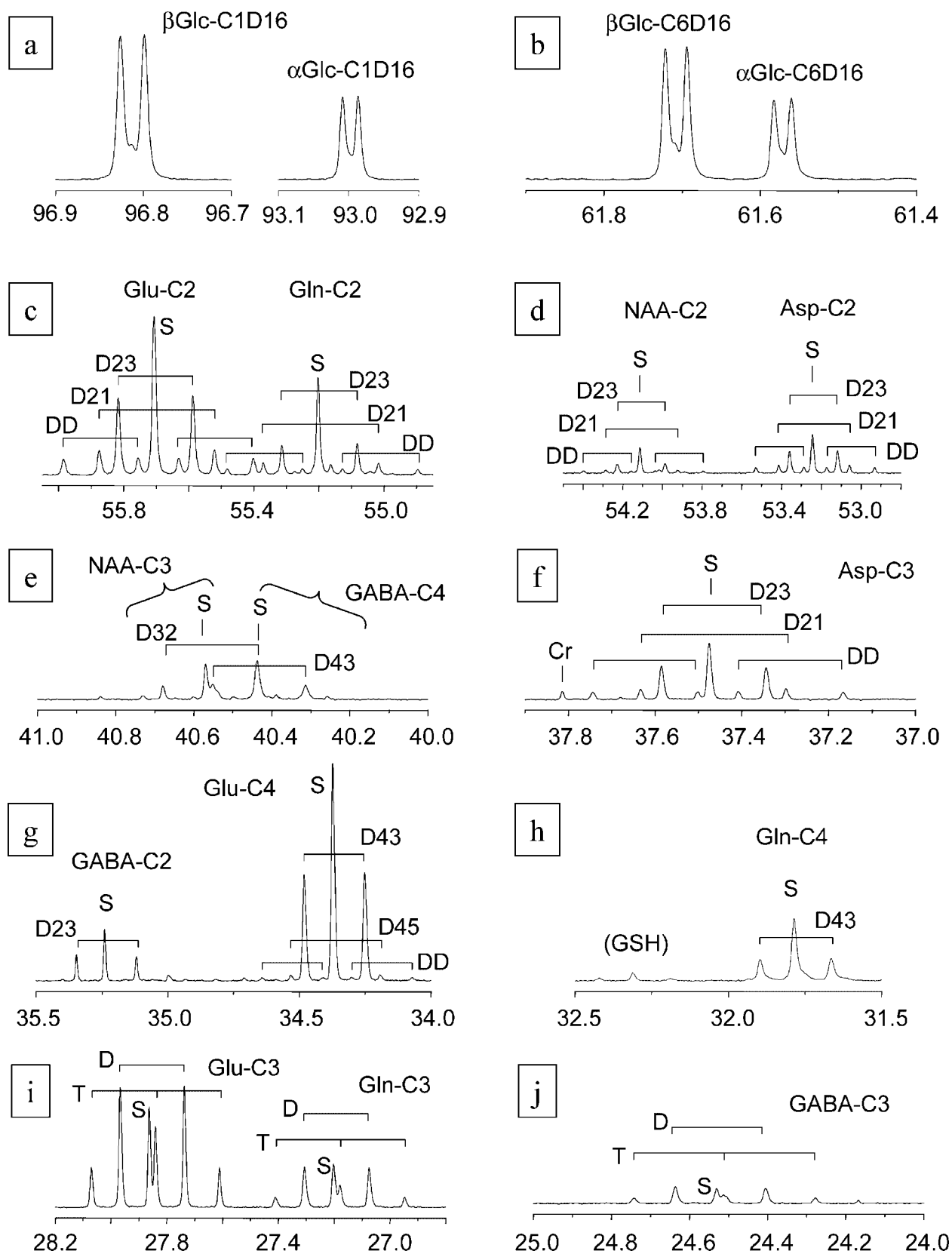


**Figure 2.** Expansions of regions from a high-resolution  $^{13}\text{C}$  spectrum of extracted rat brain tissue showing multiplets corresponding to  $^{13}\text{C}$ -labeled isotopomers: (a) glucose C1; (b) glucose C6; (c) glutamate and glutamine C2; (d) NAA and aspartate C2; (e) NAA C3 and GABA C4; (f) aspartate C3; (g) GABA C2 and glutamate C4; (h) glutamine C4 and GSH-Glu C4; (i) glutamate and glutamine C3; (j) GABA C3. Spectrum was acquired at 600 MHz (2048 scans,  $TR$  15 s, with NOE enhancement, spectral width 30 000 Hz, acquisition time 1 s). A small gaussian filtering was applied (0.3 Hz). The spectrum was acquired under *in vivo* conditions ( $\text{pH} = 7.15$ ,  $T = 37^\circ\text{C}$ )

**Table 1.** Mean chemical shifts values measured in  $^{13}\text{C}$  NMR spectra of brain extracts from five different animals. Spectra were acquired at 150 MHz under physiological conditions (pH = 7.15,  $T = 37^\circ\text{C}$ ). All chemical shifts were referenced to lactate at 21 ppm

| Resonance                 | Multiplet | Mean (ppm)<br>( $n = 5$ ) | SD (ppm)<br>( $n = 5$ ) |
|---------------------------|-----------|---------------------------|-------------------------|
| Ala-C3                    | S         | 17.13                     | 0.003                   |
| Lac-C3                    | S         | 21.00                     | 0.000                   |
| NAA-C6 (CH <sub>3</sub> ) | S         | 22.92                     | 0.001                   |
| GABA-C3                   | T         | 24.51                     | 0.002                   |
|                           | D         | 24.52                     | 0.002                   |
|                           | S         | 24.53                     | 0.002                   |
| Gln-C3                    | T         | 27.18                     | 0.012                   |
|                           | D         | 27.19                     | 0.012                   |
|                           | S         | 27.20                     | 0.012                   |
| Glu-C3                    | T         | 27.84                     | 0.005                   |
|                           | D         | 27.85                     | 0.005                   |
|                           | S         | 27.86                     | 0.005                   |
| Gln-C4                    | D43       | 31.78                     | 0.003                   |
|                           | S         | 31.79                     | 0.003                   |
| Glu-C4                    | D43       | 34.36                     | 0.004                   |
|                           | S         | 34.37                     | 0.004                   |
| GABA-C2                   | D23       | 35.23                     | 0.002                   |
|                           | S         | 35.24                     | 0.002                   |
| Asp-C3                    | DD        | 37.46                     | 0.005                   |
|                           | D32       | 37.46                     | 0.006                   |
|                           | D34       | 37.47                     | 0.006                   |
|                           | S         | 37.48                     | 0.006                   |
| Cr-CH <sub>3</sub>        | S         | 37.81                     | 0.000                   |
| GABA-C4                   | D43       | 40.43                     | 0.002                   |
|                           | S         | 40.44                     | 0.003                   |
| NAA-C3                    | D         | 40.56                     | 0.003                   |
|                           | S         | 40.57                     | 0.003                   |
| Asp-C2                    | DD        | 53.23                     | 0.003                   |
|                           | D23       | 53.24                     | 0.003                   |
|                           | D21       | 53.24                     | 0.004                   |
|                           | S         | 53.24                     | 0.003                   |
| NAA-C2                    | D23       | 54.11                     | 0.003                   |
|                           | S         | 54.11                     | 0.003                   |
| Cr-CH <sub>2</sub>        | S         | 54.75                     | 0.001                   |
| Gln-C2                    | DD        | 55.19                     | 0.005                   |
|                           | D21       | 55.19                     | 0.005                   |
|                           | D23       | 55.20                     | 0.005                   |
|                           | S         | 55.20                     | 0.005                   |
| Glu-C2                    | DD        | 55.69                     | 0.004                   |
|                           | D23       | 55.70                     | 0.004                   |
|                           | D21       | 55.70                     | 0.004                   |
|                           | S         | 55.71                     | 0.004                   |
| Serine-C3 <sup>a</sup>    | S         | 61.25                     | 0.012                   |
| Glc-C6 $\alpha$           | S,D16     | 61.57                     | 0.002                   |
| Glc-C6 $\beta$            | S,D16     | 61.71                     | 0.002                   |
| Myo-Ins C1,C3             | S         | 72.08                     | 0.002                   |
| Myo-Ins C2                | S         | 73.13                     | 0.001                   |
| Myo-Ins C4,C6             | S         | 73.38                     | 0.002                   |
| Myo-Ins C5                | S         | 75.29                     | 0.002                   |
| Glc-C1 $\alpha$           | S,D16     | 93.00                     | 0.001                   |
| Glc-C1 $\beta$            | S,D16     | 96.81                     | 0.001                   |
| NAA-C5 (C=O) <sup>b</sup> | S,D       | 174.31                    | 0.005                   |
| Gln-C1 <sup>b</sup>       | S,D       | 174.93                    | 0.019                   |
| Asp-C1 <sup>b</sup>       | S,D       | 175.06                    | 0.006                   |
| Glu-C1 <sup>b</sup>       | S,D       | 175.38                    | 0.007                   |
| Asp-C4 <sup>b</sup>       | S,D       | 178.35                    | 0.005                   |
| Gln-C5 <sup>b</sup>       | S,D       | 178.55                    | 0.007                   |
| NAA-C1 <sup>b</sup>       | S,D       | 179.49                    | 0.004                   |
| NAA-C4 <sup>b</sup>       | S,D       | 179.70                    | 0.002                   |
| Glu-C5 <sup>b</sup>       | S,D       | 182.04                    | 0.004                   |

<sup>a</sup> Assignment tentative.

<sup>b</sup> Chemical shifts of carbons in carboxyl groups provided as a reference but not included in the basis set for LCMoDel.

**Table 2.** Mean  $J$ -coupling values measured in  $^{13}\text{C}$  NMR spectra of brain extracts from five different animals. Spectra were acquired at 150 MHz under physiological conditions (pH = 7.15,  $T = 37^\circ\text{C}$ )

| Metabolite | Coupling     | Mean (Hz) | SD (Hz) |
|------------|--------------|-----------|---------|
| Glutamate  | J12          | 53.4      | 0.05    |
|            | J34, J32     | 34.6      | 0.05    |
|            | J45          | 51.3      | 0.2     |
| Glutamine  | J12          | 53.4      | 0.17    |
|            | J34, J32     | 34.9      | 0.09    |
|            | J45          | 48.4      | 0.24    |
| GABA       | J34, J32     | 35.1      | 0.38    |
| Aspartate  | J12          | 53.8      | 0.22    |
|            | J23          | 36.4      | 0.15    |
|            | J34          | 50.8      | 0.08    |
| NAA        | J12          | 54.7      | 0.13    |
|            | J23          | 36.3      | 0.22    |
|            | J34          | 51.6      | 0.05    |
|            | J56          | 50.1      | 0.10    |
| Glucose    | J16 $\beta$  | 4.1       | 0.02    |
|            | J16 $\alpha$ | 3.3       | 0.04    |

to Glu-C3D34+Glu-C3D32) and a triplet Glu-C3T [Fig. 2(i)]. The resonance frequencies of these individual components were slightly different due to isotope effects on nuclear shielding.<sup>45</sup> Chemical shifts were determined from extract spectra with a precision of 0.01 ppm (Table 1), and  $J$ -coupling values were determined with a precision below 1% (Table 2). Based on this prior knowledge of chemical-shifts and  $J$ -coupling constants, model spectra were simulated for the 50 most abundant isotopomers present in the brain after [1,6- $^{13}\text{C}_2$ ]glucose infusion. The simulation included the effect of homo-nuclear  $^{13}\text{C}$ - $^{13}\text{C}$   $J$ -evolution during DEPT as described in the Methods.

The LCMoDel fit of  $^{13}\text{C}$  spectra using this simulated basis set closely matched the *in vivo* data, as indicated by the flat residuals (Fig. 3). Even though  $^{13}\text{C}$ - $^{13}\text{C}$  multiplets were only partially resolved, the presence of multiple isotopomers was clearly observed *in vivo*. The glutamate C4 resonance was represented by a combination of a

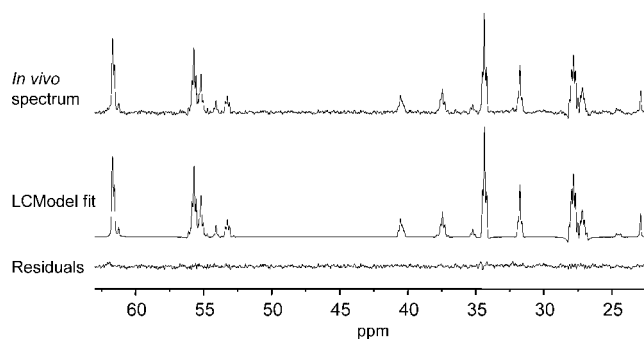


**Figure 3.** LCMoDel fit of an *in vivo*  $^{13}\text{C}$  NMR spectrum. (a)  $^1\text{H}$ -localized  $^{13}\text{C}$  spectrum acquired *in vivo* from the rat brain 5 h after starting an infusion of [1,6- $^{13}\text{C}_2$ ]glucose (2816 scans,  $TR$  2.5 s) (b) Fit obtained with LCMoDel using prior knowledge of chemical shifts and  $J$ -coupling values and (c) residuals. Only the expansion from 22 to 63 ppm is shown

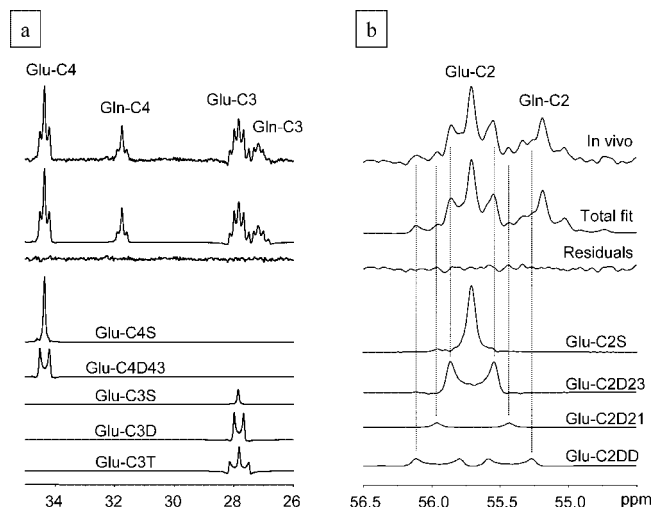


**Figure 4.** Expansions of Fig. 3 showing the fitting of individual isotopomers in glutamate and glutamine: (a) isotopomer analysis of glutamate and glutamine C4 and C3; (b) isotopomer analysis of glutamate and glutamine C2. Vertical dashed lines indicate the presence of individual isotopomers in the *in vivo* spectrum

singlet (S) and a doublet (D43) and the glutamate C3 resonance consistently contained a singlet (S), a doublet (D) and a triplet (T) resonance [Fig. 4(a)]. For glutamate C2 and glutamine C2, spectral contributions of glutamate and glutamine isotopomers (S, D23, D21, DD) were discernible with some spectral overlap between the outermost multiplet resonances even at 9.4T [Fig. 4(b)]. LCMoel analysis allowed determination of the contribution of each individual component to the *in vivo* spectrum.

To assess the reliability and robustness of the *in vivo* isotopomer distribution using LCMoel a Monte-Carlo simulation was performed using different levels of signal to rms noise ratios. These analyses showed that the determination of isotopomer concentrations remained unbiased even at signal-to-noise levels as low as 3:1 (Fig. 5). At very low sensitivity, systematic errors were apparent, but the total signal (sum of all isotopomers at a given carbon position) remained more accurate than the estimation of individual isotopomers contributions. For example, for a signal-to-noise ratio of 1, the singlet Glu-C4S was biased by 50%, but the *total* glutamate C4 signal (glu-C4S+glu-C4D43) deviated from the nominal value by only 15% on average (Fig. 5). Similar observations (not shown) were made using Monte-Carlo simulations of other multiplet structures, e.g. singlet+doublet+triplet (such as glutamate C3) or singlet+doublet1+doublet2+quartet (such as glutamate C2).

*In vivo* isotopomer analysis of glutamate, glutamine and aspartate using LCMoel was in excellent agreement with isotopomer analysis of brain extracts from the same animal (Table 3). Comparison of the *in vivo* measurement obtained immediately before funnel-freezing with the extract measurement gave a Pearson correlation

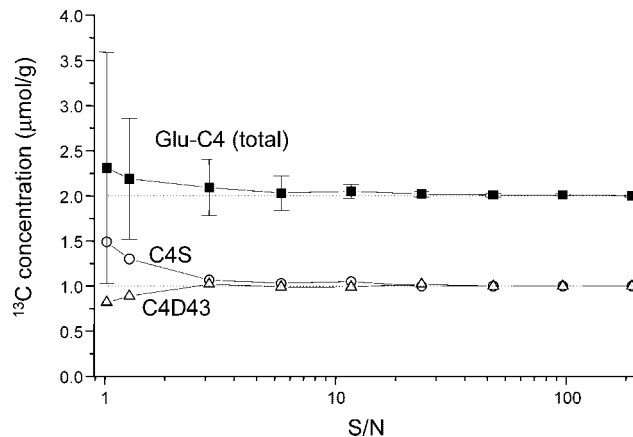


**Figure 5.** Effect of different signal-to-noise ratios on the determination of isotopomers. Shown is the result of a Monte-Carlo simulation of noise superimposed on a synthetic glutamate C4 triplet (composed of a singlet C4S and a doublet C4D43 with 1:1 ratio in signal integral, corresponding to a 50% isotopic enrichment at the C3 position), with Lorentzian lines of 8 Hz linewidth. Each point represents the result of 50 fits with a given signal-to-noise ratio (x-axis), defined as (peak height of Glu-C4S)/(2 \* rms noise)

coefficient of 0.96 ( $p < 0.001$ ) and a slope of  $1.1 \pm 0.07$  (Fig. 6), which was not significantly different from identity. Isotopomer analysis in NAA C2 and C3 and GABA C2, C3, C4 was similarly reliable when averaged over longer time periods to improve sensitivity (not shown).

The sensitivity of the experiment and concomitant LCMoel analysis indicated that the precision was sufficient to allow a temporally resolved measurement of singly and multiply labelled isotopomers *in vivo*. For example, the singlet Glu-C4S and the doublet Glu-C4D43 were measured independently with a temporal resolution of approximately 5 min [Fig. 7(A)]. The total concentration of glutamate labeled at the C4 position was obtained as the sum of these two different isotopomers (Glu-C4 = Glu-C4S + Glu-C4D43). The time course of Glu-C4D43 directly reflects the time course of  $^{13}\text{C}$  isotopic enrichment at the C3 position, as was shown in the heart.<sup>46</sup> Consistent with this, the time course of Glu-C4D43/Glu-C4 and the time course of total glutamate C3 (obtained as the sum Glu-C3S + Glu-C3D + Glu-C3T) were identical within experimental error [Fig. 7(b)]. The multiplets corresponding to glutamate labeled at the C5 position, possibly due to pyruvate recycling,<sup>24,25,47</sup> were not included in the basis set, because of their low intensity which was assessed in two animals from the C4D45 and C4DD isotopomers to be ~3% after 7 h of  $^{13}\text{C}$ -labeled glucose infusion [Fig. 2(g)].

Quantitation of time series of *in vivo* broadband localized  $^{13}\text{C}$  spectra using LCMoel resulted in the simultaneous measurement of glutamate C4, C3, C2 and glutamine C4, C3, C2 in a 400  $\mu\text{l}$  volume with a temporal resolution of 5.4 min (Fig. 8). The standard deviation of time courses at isotopic steady-state was approximately

**Table 3.** Comparison of isotopomers distribution measured *in vivo* and in extracts for glutamate, glutamine and aspartate. *In vivo* spectra were acquired at isotopic steady state immediately before funnel-freezing to allow comparison with extract spectra. The first columns give the concentration, SD, coefficient of variation, mean Cramer-Rao bound (CRB) and relative isotopomer distribution determined from five consecutive *in vivo* spectra from one animal (22 min each) using LCMoel analysis. The last column gives the relative isotopomer distribution measured in extracts spectra from the same animal

| Isotopomer   | Mean concentration<br>( $\mu\text{mol/g}$ ) | SD<br>( $\mu\text{mol/g}$ ) | CV<br>(%) | Mean CRB<br>(%) | Isotopomer<br>( <i>in vivo</i> 22 min)<br>(%) | Isotopomer<br>(extracts)<br>(%) |     |
|--------------|---|-----------------------------|-----------|-----------------|---|---------------------------------|-----|
| Glu-C4S      | 2.76  |                             | 0.08      | 3               | 3   | 53                              | 48  |
| Glu-C4D43    | 2.44  |                             | 0.11      | 4               | 4   | 47                              | 52  |
| Glu-C4 total | 5.20  |                             | 0.18      | 3               | 2   | 100                             | 100 |
| Glu-C3S      | 0.57  |                             | 0.15      | 27              | 24  | 12                              | 18  |
| Glu-C3D      | 2.31  |                             | 0.10      | 4               | 5   | 48                              | 49  |
| Glu-C3T      | 1.93  |                             | 0.15      | 8               | 10  | 40                              | 33  |
| Glu-C3 total | 4.81  |                             | 0.08      | 2               | 2   | 100                             | 100 |
| Glu-C2S      | 2.12  |                             | 0.09      | 4               | 5   | 40                              | 36  |
| Glu-C2D23    | 1.99  |                             | 0.12      | 6               | 7   | 38                              | 37  |
| Glu-C2D21    | 0.33  |                             | 0.14      | 43              | 52  | 6                               | 12  |
| Glu-C2DD     | 0.85  |                             | 0.18      | 21              | 28  | 16                              | 15  |
| Glu-C2 total | 5.29  |                             | 0.25      | 5               | 4   | 100                             | 100 |
| Gln-C4S      | 1.36  |                             | 0.07      | 5               | 6   | 63                              | 58  |
| Gln-C4D43    | 0.79  |                             | 0.06      | 7               | 12  | 37                              | 42  |
| Gln-C4 total | 2.14  |                             | 0.05      | 2               | 4   | 100                             | 100 |
| Gln-C3S      | 0.40  |                             | 0.06      | 16              | 28  | 19                              | 24  |
| Gln-C3D      | 0.92  |                             | 0.11      | 12              | 11  | 43                              | 48  |
| Gln-C3T      | 0.80  |                             | 0.26      | 32              | 24  | 38                              | 28  |
| Gln-C3 total | 2.12  |                             | 0.22      | 10              | 6   | 100                             | 100 |
| Gln-C2S      | 1.32  |                             | 0.06      | 5               | 7   | 52                              | 51  |
| Gln-C2D23    | 0.79  |                             | 0.13      | 16              | 18  | 31                              | 31  |
| Gln-C2D21    | 0.16  |                             | 0.11      | 71              | 145   | 6                               | 9   |
| Gln-C2DD     | 0.27  |                             | 0.23      | 84              | 291   | 11                              | 9   |
| Gln-C2 total | 2.54  |                             | 0.19      | 8               | 9   | 100                             | 100 |
| Asp-C2S      | 0.51  |                             | 0.07      | 15              | 17  | 37                              | 35  |
| Asp-C2D23    | 0.63  |                             | 0.07      | 11              | 20  | 47                              | 41  |
| Asp-C2D21    | 0.00  |                             | 0.00      | 0               | 999   | 0                               | 10  |
| Asp-C2DD     | 0.22  |                             | 0.09      | 43              | 94  | 16                              | 14  |
| Asp-C2 total | 1.35  |                             | 0.14      | 10              | 13  | 100                             | 100 |
| Asp-C3S      | 0.62  |                             | 0.06      | 10              | 11  | 42                              | 34  |
| Asp-C3D32    | 0.60  |                             | 0.12      | 21              | 17  | 40                              | 40  |
| Asp-C3D34    | 0.08  |                             | 0.07      | 86              | 307   | 5                               | 11  |
| Asp-C3DD     | 0.19  |                             | 0.21      | 110             | 281   | 13                              | 15  |
| Asp-C3 total | 1.48  |                             | 0.18      | 12              | 10  | 100                             | 100 |

0.2  $\mu\text{mol/g}$  at 5 min time resolution and 0.1  $\mu\text{mol/g}$  at 22 min time resolution. In addition, the incorporation of  $^{13}\text{C}$  label into glutamate C1 was measured indirectly from the corresponding isotopomers of glutamate C2, i.e. Glu-C2D21+Glu-C2DD, with a temporal resolution of 22 min [Fig. 8(b)]. The labeling time course of glutamate C1 was markedly slower than the labeling of other carbon positions, because labeling of glutamate C1 from [1,6- $^{13}\text{C}_2$ ]glucose requires  $^{13}\text{C}$  label to pass twice through the TCA cycle.

## DISCUSSION

The present study demonstrates that dynamic  $^{13}\text{C}$  isotopomer analysis is feasible in the rat brain *in vivo*. LCMoel fitting with prior knowledge of chemical-shift and *J*-coupling values, in conjunction with recent

improvements in sensitivity and resolution of  $^{13}\text{C}$  NMR spectra,<sup>8</sup> allowed the simultaneous quantitation of up to 50 different  $^{13}\text{C}$ -labeled isotopomer signals corresponding to 10 metabolites in the rat brain. This provides information that was hitherto accessible only in brain extracts.

The analysis of  $^{13}\text{C}$  NMR spectra with LCMoel required significant adaptations of the program, which was originally designed to quantify  $^1\text{H}$  spectra. These adaptations were necessary to accommodate the specific characteristics of  $^{13}\text{C}$  spectra, such as the broad spectral range and the absence of strong singlet resonances for the determination of lineshape (see Appendix). The original LCMoel method was based on the measurement of model spectra for all spin systems potentially contributing to the *in vivo* spectrum. For  $^{13}\text{C}$  NMR spectra acquired during infusion of a  $^{13}\text{C}$ -labeled substrate, the appearance of specific isotopomers requires the

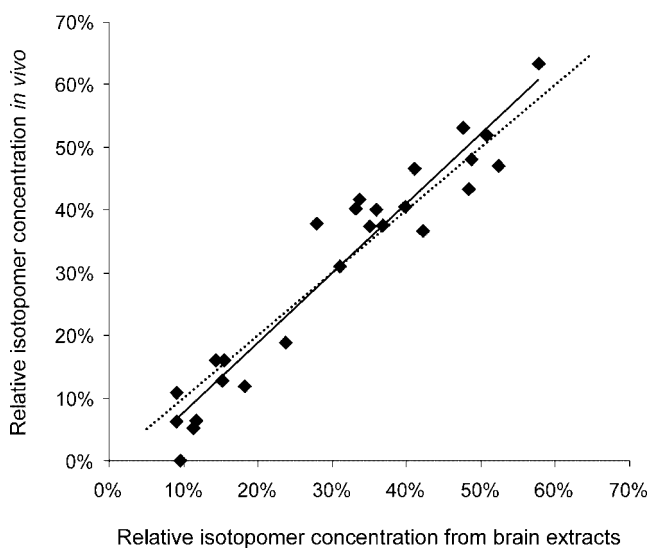


**Figure 6.** Correlation between relative isotopomer distribution measured *in vivo* and in extract. The plotted values correspond to the last two columns of Table 3. Continuous line: best linear fit to the data. Dashed line: identity

individual fit of each isotopomer signal to the spectrum, which would result in the tedious measurement of extremely expensive compounds, such as [3,4- $^{13}\text{C}_2$ ]glutamate. However, in the present study, it was possible to simulate the spectral pattern for each isotopomer, provided that *J*-couplings and chemical shifts were accurately measured.

Prior knowledge for simulating the basis set was obtained by measuring chemical-shifts and *J*-coupling constants in five animals under close to physiological conditions to minimize possible differential effects of pH and temperature on  $^{13}\text{C}$  resonances in extracts compared to *in vivo*. Overall, the values in the present study (Tables 1 and 2) were in good agreement with previously published values.<sup>24,41–43</sup> Small differences were most likely due to differences in pH and temperature conditions used to acquire extract  $^{13}\text{C}$  spectra. Interestingly, even though funnel-freezing was used in this study to minimize post-mortem changes, all three detected resonances of GABA (at 24.5, 35.2 and 40.4 ppm) were still noticeably higher in extracts than *in vivo*, consistent with other observations of a rapid increase of GABA concentration post-mortem.<sup>48</sup> This suggests that GABA levels may change even more quickly than lactate and glucose concentrations post-mortem. This was supported by comparing the present data with preliminary data obtained following focused microwave fixation of brain within 1.4 s (unpublished observation), where total tissue GABA levels were lower than with funnel-freezing.

In the present study, an information content was achieved reminiscent to what had been previously obtained only in spectra of brain extracts. For example, the isotopomer distribution was determined for glutamate C4, C3, C2, glutamine C4, C3, C2 as well as aspartate C3, C2 with a temporal resolution sufficient for dynamic

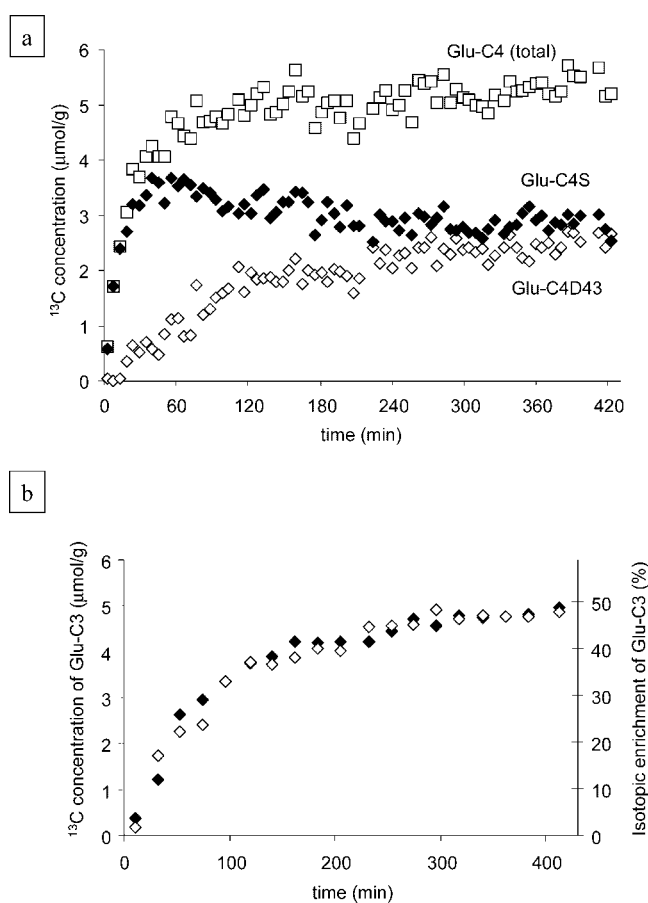


**Figure 7.** *In vivo* time courses of individual isotopomers ( $\mu\text{mol/g}$  of  $^{13}\text{C}$  label) during an infusion of [1,6- $^{13}\text{C}_2$ ]glucose: (a) Time course of Glu-C45 (solid diamonds), Glu-C4D43 (open diamonds) and total Glu-C4 (= Glu-C4S+Glu-C4D43; open squares) with a time resolution of  $\sim 5$  min (128 scans, *TR* 2.5 s); (b) comparison of C3 labeling measured directly at the C3 position (Glu-C3 = Glu-C3S+Glu-C3D+Glu-C3T; solid diamonds, left scale) or indirectly through the relative amount of doublet intensity (Glu-C4D43/Glu-C4<sub>tot</sub>) at the C4 position (open diamonds, right scale) with a time resolution of 22 min. Time courses were obtained by fitting  $^{13}\text{C}$  NMR spectra sequentially with LCMoDel

isotopomer analysis. Overall, the relative contributions of isotopomers to the total signal determined *in vivo* with LCMoDel were in excellent agreement with the isotopomer distribution measured in brain extracts (Table 3) as judged from the overlap of the data points with the identity line (Fig. 6). This determination of isotopomer distribution was very robust, even when the signal-to-noise ratio approached 3:1. To determine the isotopomer distribution in NAA and GABA required averaging data for longer time periods. The Cramer–Rao lower bounds returned by LCMoDel were very close to the coefficients of variation measured by analyzing time series of  $^{13}\text{C}$  spectra at isotopic steady state (Table 3).

The combination of FASTMAP shimming, strong second-order shim coils, and efficient spatial localization allowed consistent detection of  $^{13}\text{C}$ – $^{13}\text{C}$  couplings in the

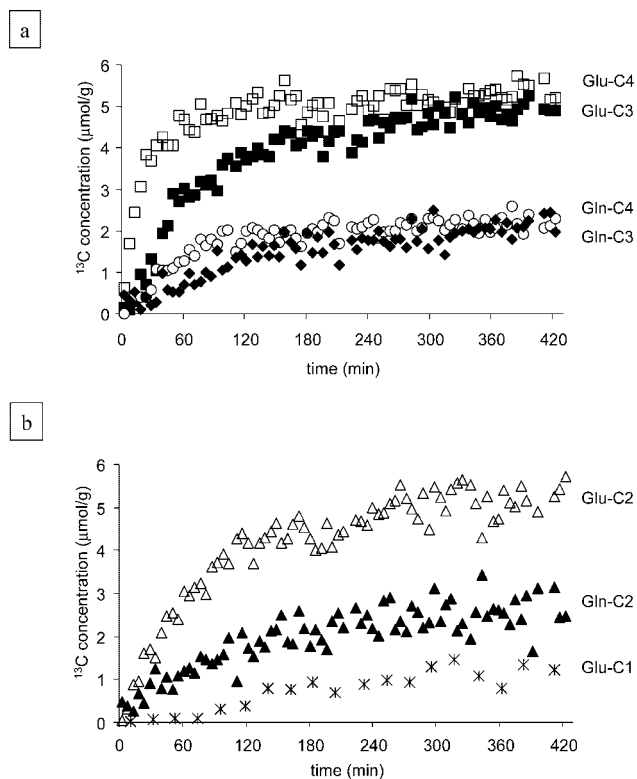


**Figure 8.** Time courses of  $^{13}\text{C}$  label incorporation into multiple carbon positions of glutamate and glutamine obtained *in vivo* from a  $400\ \mu\text{l}$  volume in the rat brain: (a) Labeling time courses of glutamate C4, glutamate C3, glutamine C4 and glutamine C3 with 5.4 min time resolution; (b) labeling time courses of glutamate C2, glutamine C2 with 5.4 min time resolution and glutamate C1 with 22 min time resolution. The labeling curves for the C4, C3 and C2 positions were obtained by adding all isotopomer signals at the corresponding carbon position (i.e.  $\text{C4} = \text{C4S} + \text{C4D43}$ ,  $\text{C3} = \text{C3S} + \text{C3D} + \text{C3T}$  and  $\text{C2} = \text{C2S} + \text{C2D23} + \text{C2D21} + \text{C2DD}$ ). The isotopic enrichment of glutamate C1 was obtained indirectly through isotopomers at the C2 position ( $\text{C1} = \text{C2D21} + \text{C2DD}$ )

brain *in vivo* in glutamate, glutamine and aspartate, as well as GABA and NAA with lower sensitivity.  $^{13}\text{C}$  singlet linewidths of 6–8 Hz full-width at half-height were significantly smaller than in most previous *in vivo* studies performed in the rat brain. However, significant overlap was still present between the different components of a multiplet within a specific carbon resonance. This spectral overlap resulted in a significant cross-correlation between some of the isotopomer signals fitted with LCModel. For example, cross-correlation between Glu-C4S and Glu-C4D43 was typically  $\sim 0.3$ , and the cross-correlation between Glu-C3S and glu-C3T was about  $\sim 0.7$ , reflecting the overlap of the singlet with the center line of the triplet (2 Hz chemical-shift difference at 150 MHz). The precision on the fit of the *sum* of all isotopomers contributions to a specific carbon position (e.g.  $\text{C3S} + \text{C3D} + \text{C3T}$ ) was systematically better than the precision of the fit of individual components (Fig. 5), indicating that the sum of all isotopomers can be

measured reliably even when sensitivity does not allow the precise quantitation of individual components of a multiplet (Table 3). In cases where the signal-to-noise ratio is not sufficient to measure low intensity isotopomers, selective homonuclear  $^{13}\text{C}$  decoupling could be applied to improve signal-to-noise ratio and spectral resolution as shown in the intact perfused heart,<sup>49</sup> by collapsing, for example, the nine line glutamate C2 multiplet into a pseudo-triplet.

As pointed out previously, relative isotopomer concentrations are not a direct measure of the isotopic enrichment.<sup>50</sup> However, from the isotopomers, the isotopic enrichment can be calculated. For example, the ratio  $\text{C4D43}/(\text{C4S} + \text{C4D43})$  is equal to the isotopic enrichment of the C3 carbon position in glutamate and glutamine (assuming no labeling at the C5 position). Similarly, the isotopic enrichment of the C2 and C4,  $\text{IE}_{\text{C2}}$  and  $\text{IE}_{\text{C4}}$ , respectively, can be calculated from the C3 multiplet, as follows: the probabilities of obtaining double and triply labeled isotopomers are  $\text{C3D} = \text{IE}_{\text{C2}} \cdot (1 - \text{IE}_{\text{C4}}) + \text{IE}_{\text{C4}} \cdot (1 - \text{IE}_{\text{C2}})$  and  $\text{C3T} = \text{IE}_{\text{C2}} \cdot \text{IE}_{\text{C4}}$  respectively, from which  $\text{IE}_{\text{C2}} \cdot \text{IE}_{\text{C4}} = \text{C3T}$  and  $\text{IE}_{\text{C2}} + \text{IE}_{\text{C4}} = \text{C3D} + 2 \cdot \text{C3T}$  can be obtained. These two equations with two unknowns,  $\text{IE}_{\text{C2}}$  and  $\text{IE}_{\text{C4}}$ , can be solved, but the solutions cannot be assigned unambiguously to either the C2 or the C4 isotopic enrichment unless additional information is obtained (e.g. which resonance has the highest total signal). Such an *in vivo* measurement of  $^{13}\text{C}$  isotopic enrichment is highly desirable in human studies, where extracts cannot be obtained. Measurement of isotopic enrichments *in vivo* normally requires the additional acquisition of  $^1\text{H}$ - $^{13}\text{C}$  edited spectra, the quantitation of which may be complicated by severe spectral overlap. In addition, isotopic enrichments obtained from  $^1\text{H}$ - $^{13}\text{C}$  NMR spectra may be biased by the presence of metabolically inert pools.

The standard deviation of  $^{13}\text{C}$  concentrations measured at isotopic steady state from a  $400\ \mu\text{l}$  volume was on average  $0.1\ \mu\text{mol/g}$  with 22 min time resolution (Table 3). In the presence of spectral overlap, such as glutamate C2 and glutamine C2, the standard deviations were slightly higher, reflecting the cross-correlation between overlapping signals. The measured standard deviations confirm that labeling time courses of glutamate ( $\sim 5\ \mu\text{mol/g}$  of label at isotopic steady state in this study) and glutamine ( $\sim 2\ \mu\text{mol/g}$  of label) can be measured reliably with a temporal resolution as low as 5 min (standard deviation  $0.2\ \mu\text{mol/g}$ ), and aspartate ( $\sim 1.5\ \mu\text{mol/g}$  of label) with a time resolution of 22 min (standard deviation  $0.1\ \mu\text{mol/g}$ ). This also implies that GABA time courses ( $^{13}\text{C}$  concentration  $\sim 0.25\ \mu\text{mol/g}$  at isotopic steady state) can be obtained with a temporal resolution of  $\sim 1\ \text{h}$ , which was confirmed experimentally (not shown). Further improvements in the quantification of time series of  $^{13}\text{C}$  spectra should be possible by taking into account the common information present in all spectra of the time series, similar to a recent study,<sup>21</sup> provided that such an

approach accommodates small line shape and line width changes that can occur *in vivo*.

The excellent sensitivity of  $^{13}\text{C}$  NMR spectra in our study and the robustness of LCModel analysis to quantify total  $^{13}\text{C}$  label at a given carbon position also predicted that  $^{13}\text{C}$  labeling time courses for glutamate and glutamine could be measured with excellent sensitivity from a small volume. Consistent with this, time courses of  $^{13}\text{C}$  label incorporation into glutamate and glutamine C4 and C3 were measured in the rat somatosensory cortex ( $8 \times 2 \times 3$  mm) with a time resolution of 11 min (data not shown). The signal-to-noise ratio of  $^{13}\text{C}$  NMR signals from this 48  $\mu\text{l}$  volume was 8:1 and 3:1 for glutamate C4 and glutamine C4 at isotopic steady state. After quantitation with LCModel, the standard deviation of total  $^{13}\text{C}$  concentration at the glutamate and glutamine C4 and C3 carbon positions was approximately 0.4 mM at isotopic steady-state, corresponding to a coefficient of variation of 8% for glutamate and 20% for glutamine. This demonstrates the feasibility of measuring  $^{13}\text{C}$  labeling time courses from small, localized areas of the rat brain using *direct*  $^{13}\text{C}$  NMR spectroscopy.

Most metabolic studies have derived metabolic fluxes in the brain based only on one or two  $^{13}\text{C}$  labeling time courses e.g. glutamate C4 alone,<sup>51</sup> glutamate C4 and glutamate C3<sup>34,52,53</sup> or glutamate C4 and glutamine C4.<sup>12,13</sup> Recent studies have suggested that including more information in the modeling of brain metabolism provides results that depend on fewer assumptions.<sup>5,10,34</sup> For example, it has been reported by several groups that the exchange rate between 2-oxoglutarate and glutamate,  $V_x$ , is low (on the order of the flux through pyruvate dehydrogenase  $V_{\text{pdh}}$ ) in the brain,<sup>5,10,34</sup> as it is in the heart<sup>54</sup> and liver.<sup>27</sup> Therefore, the rate of label incorporation into the C4 carbon position of glutamate alone may not be adequate to measure  $V_{\text{pdh}}$ . Similarly, detection of the C2 labeling can be used to estimate the anaplerotic flux through pyruvate carboxylase.<sup>5,7,55,56</sup> In general, with increased information and decreased assumptions used for the modeling, metabolic fluxes can be determined more accurately.<sup>57</sup>

## CONCLUSION

In conclusion, high-field localized  $^{13}\text{C}$  NMR spectroscopy combined with LCModel analysis permits us to obtain *in vivo* a wealth of metabolic information hitherto available only in extracts. This is expected to provide novel information to measure quantitative metabolic fluxes and further investigate compartmentalized metabolism in the brain.

## APPENDIX: ADAPTATIONS OF THE LCMODEL PROGRAM TO ANALYZE $^{13}\text{C}$ NMR SPECTRA

A modified version of LCModel v2.3 was necessary to accommodate the larger number of points of  $^{13}\text{C}$  spectra

and the higher number of metabolites in the basis set compared with  $^1\text{H}$  spectra. Specifically, LCModel 2.3 normally allows a maximum of 4096 complex points in FIDs, a maximum spectral range of 2000 complex points for the fit, and a maximum of 40 metabolites in the basis set. The modified version accepted FIDs with up to 8192 complex points, allowed to fit a spectral range of 4000 complex points, and incorporated up to 60 metabolites in the basis set.

In addition, several parameters provided in the CONTROL input file had to be modified, some of which are not described in the documentation of LCModel:

- The knot spacing for the spline baseline function, DKNTMN was set to the maximum value (DKNTMN = 2\*99) to impose a flat baseline in the fit.
- To prevent the pseudo-triplets from getting mistaken for a single resonance in the estimation of the line shape, the parameter NSIDMN that specifies the minimum number of grid points on each side of the line-shape (default value = 5) was reduced to 2.
- The estimated linewidth of the (simulated) basis spectra, FWHMBA, was set to 0.049.
- One major difference between  $^1\text{H}$  and  $^{13}\text{C}$  spectra is the  $\sim 30$  fold change in ppm range. The modifications ALPBMN = 108, ALPBMX = 54000, ALPBPN = 135, ALPBST = 162 reflect this difference in ppm range. The proposed values of these parameters are about  $(30)^3$  times their default  $^1\text{H}$  value. The 30-fold increase in ppm range would require many additional changes in the LCModel program unless the knot spacing is fixed to a large value with DKNTMN and phase parameters are set close to their optimal value with DEGZER and DEGPPM.
- More freedom was given to LCModel to allow small frequency shifts between the *in vivo* data and the basis set by setting DESDSH to 0.01 (in ppm) rather than the default 0.004 value used for  $^1\text{H}$ .
- Estimation of the lineshape was performed on the glucose C1, glucose C6, glutamate C4S, glutamate C4D43, NAA C6, specified by NUSE1 and CHUSE1. Including the doublet (e.g. Glu-C4D43) together with the singlet (e.g. Glu-C4S) minimized the occurrence of errors in the line shape analysis caused by overlap between the singlet and the doublet.
- The phase of the spectra was determined manually on the sum of the entire time course (the phase was stable over the entire time course) and starting values for DEGZER and DEGPPM were entered (DEGZER =  $-\text{rp} - 0.5 * \text{lp}$  and DEGPPM =  $-\text{lp} / (\text{spectral width in ppm})$ , where rp and lp are the Varian parameters for zero and first order phase adjustment). Small degrees of freedom were left to both zero and first order phase by setting SDDEGZ = 3 and SDDEGP = 0.5.
- NCOMBI, CHCOMB: combination used to obtain the sums of isotopomers at a given carbon position, e.g. CHCOMB(1) = "gluC3+gluC34+glu324" gives the

total concentration and Cramer–Rao bound for total glutamate C3.

## Acknowledgments

We thank Sarah Crawford and Kevin Yue for expert technical assistance, and Dr Ivan Tkáč for useful discussions. This work was supported by NIH grant R01NS38672 (R.G.) and the Whitaker Foundation (R.G.). The Center for Magnetic Resonance Research was supported in part by NIH grant P41RR08079. The 9.4 T/31 cm spectrometer was purchased in part with a grant from the Keck Foundation. P.G.H. was supported in part by a Lavoisier grant from the French Foreign Affairs Ministry. The high-resolution NMR facility was supported by funds from the NSF (BIR-961477), the University of Minnesota Medical School, and the Minnesota Medical Foundation.

## REFERENCES

- Bachelard H. Landmarks in the application of  $^{13}\text{C}$ -magnetic resonance spectroscopy to studies of neuronal/glial relationships. *Dev. Neurosci.* 1998; **20**: 277–288.
- Cruz F, Cerdan S. Quantitative  $^{13}\text{C}$  NMR studies of metabolic compartmentation in the adult mammalian brain. *NMR Biomed.* 1999; **12**: 451–462.
- Gruetter R, Adriany G, Merkle H, Andersen PM. Broadband decoupled,  $^1\text{H}$ -localized  $^{13}\text{C}$  MRS of the human brain at 4 Tesla. *Magn. Reson. Med.* 1996; **36**: 659–664.
- Gruetter R, Seaquist ER, Kim S, Ugurbil K. Localized *in vivo*  $^{13}\text{C}$ -NMR of glutamate metabolism in the human brain: initial results at 4 Tesla. *Dev. Neurosci.* 1998; **20**: 380–388.
- Gruetter R, Seaquist ER, Ugurbil K. A mathematical model of compartmentalized neurotransmitter metabolism in the human brain. *Am. J. Physiol.* 2001; **281**: E100–E112.
- Shen J, Petersen KF, Behar KL, Brown P, Nixon TW, Mason GF, Petroff OAC, Shulman GI, Shulman RG, Rothman DL. Determination of the rate of the glutamate/glutamine cycle in the human brain by *in vivo*  $^{13}\text{C}$  NMR. *Proc. Natl Acad. Sci. USA* 1999; **96**: 8235–8240.
- Lebon V, Petersen KF, Cline GW, Shen J, Mason GF, Dufour S, Behar KL, Shulman GI, Rothman DL. Astroglial contribution to brain energy metabolism in humans revealed by  $^{13}\text{C}$  nuclear magnetic resonance spectroscopy: elucidation of the dominant pathway for neurotransmitter glutamate repletion and measurement of astrocytic oxidative metabolism. *J. Neurosci.* 2002; **22**: 1523–1531.
- Henry P-G, Tkac I, Gruetter R.  $^1\text{H}$ -localized broadband  $^{13}\text{C}$  NMR spectroscopy of the rat brain *in vivo* at 9.4 Tesla. *Magn. Reson. Med.* 2003; **50**(4): 684–692.
- Choi IY, Tkac I, Gruetter R. Single-shot three-dimensional 'non-echo' localization method for *in vivo* NMR spectroscopy. *Magn. Reson. Med.* 2000; **44**: 387–394.
- Choi IY, Lei HX, Gruetter R. Effect of deep pentobarbital anesthesia on neurotransmitter metabolism *in vivo*: on the correlation of total glucose consumption with glutamatergic action. *J. Cereb. Blood Flow Metab.* 2002; **22**: 1343–1351.
- Gruetter R, Tkac I. Field mapping without reference scan using asymmetric echo-planar techniques. *Magn. Reson. Med.* 2000; **43**: 319–323.
- Sibson NR, Dhankhar A, Mason GF, Behar KL, Rothman DL, Shulman RG. *In vivo*  $^{13}\text{C}$  NMR measurements of cerebral glutamine synthesis as evidence for glutamate–glutamine cycling. *Proc. Natl Acad. Sci. USA* 1997; **94**: 2699–2704.
- Sibson NR, Dhankhar A, Mason GF, Rothman DL, Behar KL, Shulman RG. Stoichiometric coupling of brain metabolism and glutamatergic neuronal activity. *Proc. Natl Acad. Sci. USA* 1998; **95**: 316–321.
- de Graaf AA, Bovee WM. Improved quantification of *in vivo*  $^1\text{H}$  NMR spectra by optimization of signal acquisition and processing and by incorporation of prior knowledge into the spectral fitting. *Magn. Reson. Med.* 1990; **15**: 305–319.
- van Dijk JE, Mehlkopf AF, van Ormondt D, Bovee WM. Determination of concentrations by time domain fitting of proton NMR echo signals using prior knowledge. *Magn. Reson. Med.* 1992; **27**: 76–96.
- Cavassila S, Deval S, Huegen C, van Ormondt D, Graveron-Demilly D. Cramer-Rao bound expressions for parametric estimation of overlapping peaks: influence of prior knowledge. *J. Magn. Reson.* 2000; **143**: 311–320.
- Vanhamme L, Sundin T, Hecke PV, Huffel SV. MR spectroscopy quantitation: a review of time-domain methods. *NMR Biomed.* 2001; **14**: 233–246.
- Mierisova S, Ala-Korpela M. MR spectroscopy quantitation: a review of frequency domain methods. *NMR Biomed.* 2001; **14**: 247–259.
- Laatikainen R, Niemitz M, Malaisse WJ, Biesemans M, Willem R. A computational strategy for the deconvolution of NMR spectra with multiplet structures and constraints: analysis of overlapping  $^{13}\text{C}$ - $^2\text{H}$  multiplets of  $^{13}\text{C}$  enriched metabolites from cell suspensions incubated in deuterated media. *Magn. Reson. Med.* 1996; **36**: 359–365.
- Vanhamme L, van den Boogaart A, Van Huffel S. Improved method for accurate and efficient quantification of MRS data with use of prior knowledge. *J. Magn. Reson.* 1997; 35–43.
- Vanhamme L, Van Huffel S, Van Hecke P, van Ormondt D. Time-domain quantification of series of biomedical magnetic resonance spectroscopy signals. *J. Magn. Reson.* 1999; **140**: 120–130.
- van der Veen JW, de Beer R, Luyten PR, van Ormondt D. Accurate quantification of *in vivo*  $^{31}\text{P}$  NMR signals using the variable projection method and prior knowledge. *Magn. Reson. Med.* 1988; **6**: 92–98.
- Provencher S. Estimation of metabolite concentrations from localized *in vivo* proton NMR spectra. *Magn. Reson. Med.* 1993; **30**: 672–679.
- Cerdan S, Kunnecke B, Seelig J. Cerebral metabolism of  $[1,2\text{-}^{13}\text{C}_2]$ acetate as detected by *in vivo* and *in vitro*  $^{13}\text{C}$  NMR. *J. Biol. Chem.* 1990; **265**: 12916–12926.
- Kunnecke B, Cerdan S, Seelig J. Cerebral metabolism of  $[1,2\text{-}^{13}\text{C}_2]$ glucose and  $[U\text{-}^{13}\text{C}_4]$ 3-hydroxybutyrate in rat brain as detected by  $^{13}\text{C}$  NMR spectroscopy. *NMR Biomed.* 1993; **6**: 264–277.
- Jeffrey FM, Storey CJ, Sherry AD, Malloy CR.  $^{13}\text{C}$  isotopomer model for estimation of anaplerotic substrate oxidation via acetyl-CoA. *Am. J. Physiol.* 1996; **271**: E788–E799.
- Garcia-Martin ML, Garcia-Espinosa MA, Ballesteros P, Bruix M, Cerdan S. Hydrogen turnover and subcellular compartmentation of hepatic  $[2\text{-}(13)\text{C}]$ glutamate and  $[3\text{-}(13)\text{C}]$ aspartate as detected by  $(13)\text{C}$  NMR. *J. Biol. Chem.* 2002; **277**: 7799–7807.
- Slotboom J, Boesch C, Kreis R. Versatile frequency domain fitting using time domain models and prior knowledge. *Magn. Reson. Med.* 1998; **39**: 899–911.
- Bergans N, Dresselaers T, Vanhamme L, Van Hecke P, Van Huffel S, Vanstapel F. Quantification of the glycogen  $^{13}\text{C}$ -1 NMR signal during glycogen synthesis in perfused rat liver. *NMR Biomed.* 2003; **16**: 36–46.
- Provencher, SW. Automatic quantitation of localized *in vivo*  $^1\text{H}$  spectra with LCModel. *NMR Biomed.* 2001; **14**: 260–264.
- Pfeuffer J, Tkac I, Provencher SW, Gruetter R. Toward an *in vivo* neurochemical profile: quantification of 18 metabolites in short-echo-time  $(1)\text{H}$  NMR spectra of the rat brain. *J. Magn. Reson.* 1999; **141**: 104–120.
- Tkac I, Keene CD, Pfeuffer J, Low WC, Gruetter R. Metabolic changes in quinolinic acid-lesioned rat striatum detected non-invasively by *in vivo*  $(1)\text{H}$  NMR spectroscopy. *J. Neurosci. Res.* 2001; **66**: 891–898.
- Terpstra M, Henry P-G, Gruetter R. Measurement of reduced glutathione (GSH) in human brain using LCModel analysis of difference-edited spectra. *Magn. Reson. Med.* 2003; **50**: 19–23.

34. Henry P-G, Lebon V, Vaufrey F, Brouillet E, Hantraye P, Bloch G. Decreased TCA cycle rate in the rat brain after acute 3-NP treatment measured by *in vivo*  $^1\text{H}$ - $^{13}\text{C}$  NMR spectroscopy. *J. Neurochem.* 2002; **82**: 857–866.
35. Adriany G, Gruetter R. A half-volume coil for efficient proton decoupling in humans at 4 Tesla. *J. Magn. Reson.* 1997; **125**: 178–184.
36. Ponten U, Ratcheson RA, Salford LG, Siesjo BK. Optimal freezing conditions for cerebral metabolites in rats. *J. Neurochem.* 1973; **21**: 1127–1138.
37. Cruz NF, Dienel GA. High glycogen levels in brains of rats with minimal environmental stimuli: implications for metabolic contributions of working astrocytes. *J. Cereb. Blood Flow Metab.* 2002; **22**: 1476–1489.
38. Kintner DB, Anderson ME, Sailor KA, Dienel G, Fitzpatrick JH, Jr., Gilboe DD. *In vivo* microdialysis of 2-deoxyglucose 6-phosphate into brain: a novel method for the measurement of interstitial pH using  $^{31}\text{P}$ -NMR. *J. Neurochem.* 1999; **72**: 405–412.
39. Glasoe PK, Long FA. Use of glass electrodes to measure acidities in deuterium oxide. *Journal of Physical Chemistry* 1960; **64**: 188–190.
40. Willker W, Engelmann J, Brand A, Leibfritz D. Metabolite identification in cell extracts and culture media by proton-detected 2D- $^1\text{H}$ , $^{13}\text{C}$ -NMR spectroscopy. *J. Magn. Reson. Anal.* 1996; **2**: 21–32.
41. London RE.  $^{13}\text{C}$  labeling in studies of metabolic regulation. *Prog. Nucl. Magn. Reson. Spectrosc.* 1988; **20**: 337–383.
42. Barany M, Arus C, Chang YC. Natural-abundance  $^{13}\text{C}$  NMR of brain. *Magn. Reson. Med.* 1985; **2**: 289–295.
43. Bluml S, Hwang JH, Moreno A, Ross BD. Novel peak assignments of *in vivo* ( $^{13}\text{C}$ ) MRS in human brain at 1.5 T. *J. Magn. Reson.* 2000; **143**: 292–298.
44. Carvalho RA, Babcock EE, Jeffrey FM, Sherry AD, Malloy CR. Multiple bond  $^{13}\text{C}$ – $^{13}\text{C}$  spin–spin coupling provides complementary information in a  $^{13}\text{C}$  NMR isotopomer analysis of glutamate. *Magn. Reson. Med.* 1999; **42**: 197–200.
45. Hansen RE. Isotope effects in nuclear shielding. *Prog. Nucl. Magn. Reson. Spectrosc.* 1988; **20**: 207–255.
46. Jeffrey FM, Reshetov A, Storey CJ, Carvalho RA, Sherry AD, Malloy CR. Use of a single ( $^{13}\text{C}$ ) NMR resonance of glutamate for measuring oxygen consumption in tissue. *Am. J. Physiol.* 1999; **277**: E1111–E1121.
47. Haberg A, Qu H, Bakken IJ, Sande LM, White LR, Haraldseth O, Unsgard G, Aasly J, Sonnewald U. *In vitro* and *ex vivo*  $^{13}\text{C}$ -NMR spectroscopy studies of pyruvate recycling in brain. *Dev. Neurosci.* 1998; **20**: 389–398.
48. Hanstock CC, Coupland NJ, Allen PS. GABA X2 multiplet measured pre- and post-administration of vigabatrin in human brain. *Magn. Reson. Med.* 2002; **48**: 617–623.
49. Sherry AD, Zhao P, Wiethoff A, Malloy CR.  $^{13}\text{C}$  isotopomer analyses in intact tissue using  $^{13}\text{C}$  homonuclear decoupling. *Magn. Reson. Med.* 1994; **31**: 374–379.
50. Malloy CR, Sherry AD, Jeffrey FM. Analysis of tricarboxylic acid cycle of the heart using  $^{13}\text{C}$  isotope isomers. *Am. J. Physiol.* 1990; **259**: H987–995.
51. Mason GF, Pan JW, Chu W-J, Newcomer BR, Zhang Y, Orr R, Hetherington HP. Measurement of the tricarboxylic acid cycle rate in human grey and white matter *in vivo* by  $^1\text{H}$ - $^{13}\text{C}$  magnetic resonance spectroscopy at 4.1 T. *J. Cereb. Blood Flow Metab.* 1999; **19**: 1179–1188.
52. Mason GF, Rothman DL, Behar KL, Shulman RG. NMR determination of the TCA cycle rate and a-ketoglutarate/glutamate exchange rate in rat brain. *J. Cereb. Blood Flow Metab.* 1992; **12**: 434–447.
53. Mason GF, Gruetter R, Rothman DL, Behar KL, Shulman RG, Novotny EJ. Simultaneous determination of the rates of the TCA cycle, glucose utilization,  $\alpha$ -ketoglutarate/glutamate exchange, and glutamine synthesis in human brain by NMR. *J. Cereb. Blood Flow Metab.* 1995; **15**: 12–25.
54. Yu X, Alpert NM, Lewandowski ED. Modeling enrichment kinetics from dynamic  $^{13}\text{C}$ -NMR spectra: theoretical analysis and practical considerations. *Am. J. Physiol.* 1997; **272**: C2037–2048.
55. Lapidot A, Gopher A. Cerebral metabolic compartmentation. Estimation of glucose flux via pyruvate carboxylase/pyruvate dehydrogenase by  $^{13}\text{C}$  NMR isotopomer analysis of D-[U- $^{13}\text{C}$ ]glucose metabolites. *J. Biol. Chem.* 1994; **269**: 27198–27208.
56. Sibson NR, Mason GF, Shen J, Cline GW, Herskovits AZ, Wall JE, Behar KL, Rothman DL, Shulman RG. *In vivo*  $^{13}\text{C}$  NMR measurement of neurotransmitter glutamate cycling, anaplerosis and TCA cycle flux in rat brain during [2- $^{13}\text{C}$ ]glucose infusion. *J. Neurochem.* 2001; **76**: 975–989.
57. Gruetter R. *In vivo*  $^{13}\text{C}$  NMR studies of compartmentalized cerebral carbohydrate metabolism. *Neurochem. Int.* 2002; **41**: 143–154.